

# Generalized Event Partonomy Inference with Structured Hierarchical Predictive Learning

Zhou Chen, Joe Lin, Sathyanarayanan N. Aakur  
 CSSE Department, Auburn University  
 Auburn, AL, 36849  
 {zzc0053, jz10277, san0028}@auburn.edu

## Abstract

Humans naturally perceive continuous experience as a hierarchy of temporally nested events, fine-grained actions embedded within coarser routines. Replicating this structure in computer vision requires models that can segment video not just retrospectively, but predictively and hierarchically. We introduce *PARSE*, a unified framework that learns multi-scale event structure directly from streaming video without supervision. *PARSE* organizes perception into a hierarchy of recurrent predictors, each operating at its own temporal granularity: lower layers model short-term dynamics while higher layers integrate longer-term context through attention-based feedback. Event boundaries emerge naturally as transient peaks in prediction error, yielding temporally coherent, nested partonomies that mirror the containment relations observed in human event perception. Evaluated across three benchmarks, *Breakfast Actions*, *50 Salads*, and *Assembly 101*, *PARSE* achieves state-of-the-art performance among streaming methods and rivals offline baselines in both temporal alignment (*H-GEED*) and structural consistency (*TED*, *hF1*). The results demonstrate that predictive learning under uncertainty provides a scalable path toward human-like temporal abstraction and compositional event understanding. Code and evaluation tools will be released publicly upon acceptance.

## 1. Introduction

Humans experience the world not as a sequence of frames, but as a *structured stream of events* unfolding across *multiple timescales*. When we observe a person making breakfast, we perceive fine-grained actions such as “*crack egg*” and “*pour milk*” as parts of broader routines, like “*make omelet*” or “*prepare breakfast*”. This nested organization, known as a *partonomy*, is fundamental to how perception, memory, and action interact over time. An example is shown in Figure 1. Cognitive and neuroscien-



Figure 1. **Hierarchical Event Partonomy.** Real-world activities unfold across multiple temporal and semantic scales, from long-horizon tasks (L4) decomposed into goals (L3), activities (L2), and atomic actions (L1). Each higher-level subsumes several temporally contained subevents, forming a structured partonomy.

tific theories [58, 59, 65, 66] suggest that such structure emerges from predictive processing: the brain continually anticipates what happens next, updating internal hypotheses when prediction errors spike. This dynamic coupling of anticipation and reorganization allows humans to segment continuous experience into hierarchically contained events.

Despite significant progress in temporal segmentation and activity recognition [3, 9, 22, 36, 51, 53, 63, 64], most computer vision models treat event understanding as a flat or retrospective segmentation and labeling problem. Supervised methods [28, 49, 61] rely on pre-defined action boundaries and labels, while unsupervised [1, 3, 44, 45] or clustering-based approaches [38, 49] segment videos post hoc using global heuristics. These formulations lack the streaming, predictive, and hierarchical characteristics of human perception. They treat segmentation as an after-the-fact optimization rather than an emergent property of how agents anticipate and interpret unfolding experience, resulting in inconsistent boundaries across temporal scales and no notion of *hierarchical containment*.

We propose *PARSE*, a hierarchical predictive learning

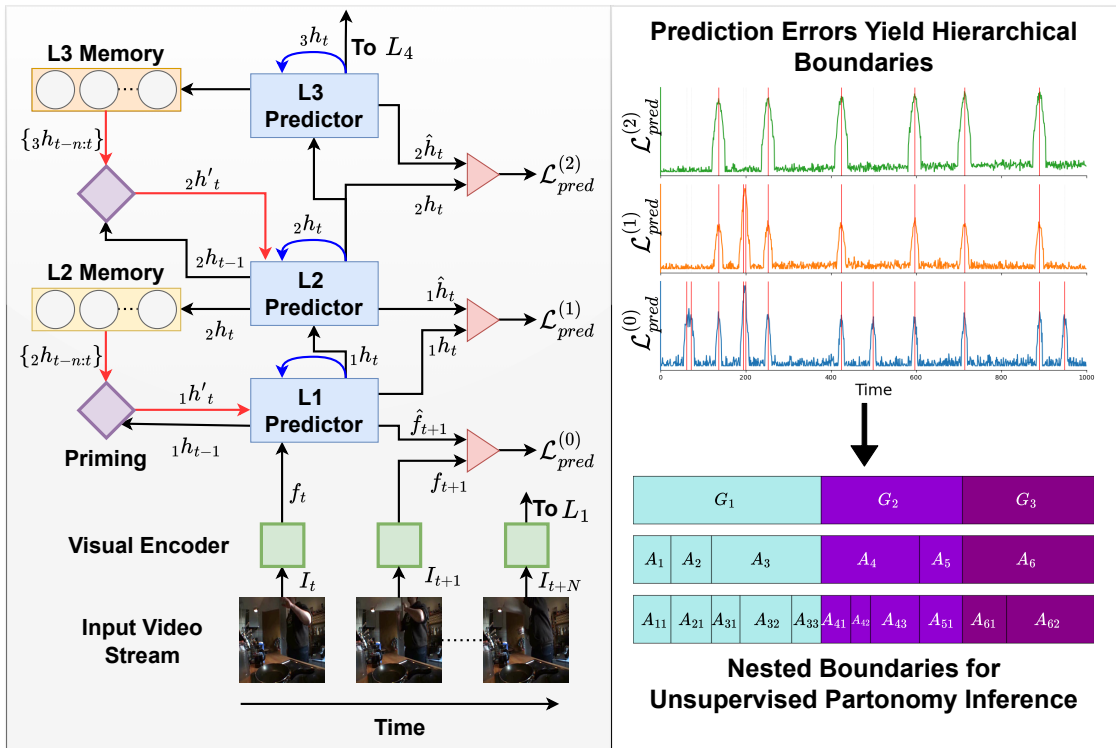


Figure 2. **PARSE Architecture Overview.** At each timestep, the visual encoder extracts frame-level features ( $f_t$ ) that feed into a hierarchy of recurrent predictors ( $L_1, L_2, L_3 \dots L_N$ ), each modeling temporal dynamics at a distinct scale. Each predictor generates a forward estimate ( $\hat{h}_t^{(i)}$ ) of its lower-level hidden state ( $h_t^{(i-1)}$ ) and computes a prediction error loss ( $\mathcal{L}_{pred}^{(i)}$ ). Transient peaks in these hierarchical prediction errors (right) signal event transitions at progressively coarser temporal scales. Aggregating these peaks yields *nested event boundaries*, which form a partonomic structure capturing the coarse-to-fine organization of real-world activities.

framework that infers multiscale event structure directly from streaming video. Figure 2 illustrates the overall process. Instead of detecting boundaries explicitly, PARSE learns to anticipate future perceptual states at multiple temporal resolutions and reorganizes its internal hypotheses when prediction errors accumulate. Each layer functions as a recurrent predictor operating at its own temporal granularity, with higher layers integrating longer-term dynamics and modulating lower layers through top-down attention. This interplay between bottom-up prediction and top-down contextualization yields temporally aligned, nested boundaries that naturally form a partonomic hierarchy.

Our **contributions** are four-fold: (1) We introduce a formal definition and computational model of hierarchical partonomy inference, framing event segmentation as a process of predictive reorganization. (2) We develop PARSE, a multi-layer predictive hierarchy that unifies anticipation, sparsity-driven stability, and hierarchical boundary extraction under a single energy-based objective. (3) We propose an unsupervised boundary inference mechanism that iden-

tifies multi-scale transitions from prediction-error dynamics during streaming inference. (4) We establish evaluation benchmarks for hierarchical event understanding, combining boundary-level (H-GEBD) and structural (TED, hF1) metrics across three datasets, Breakfast Actions [36], 50 Salads [54], and Assembly101 [51].

## 2. Related Work

**Predictive learning** conceptualizes perception as an anticipatory process in which internal models continually generate expectations about future sensory input and update their hypotheses when predictions fail. Rooted in cognitive science and neuroscience [15, 23, 42, 43, 47], it posits that perception and attention emerge from minimizing prediction error across hierarchical cortical pathways. Empirical studies of event perception [58, 65] show that humans segment continuous experience at moments of heightened prediction error, suggesting that event boundaries mark points where generative models of the world are revised. Hierarchical predictive inference [32, 46–48] suggests that stable,

long-timescale representations can emerge from nested predictive processes. In computer vision, this idea has been explored through self-supervised representation learning. Early work [3, 62] modeled event segmentation through prediction-error dynamics, while subsequent efforts provide extensions to active control [13, 56] and online localization [1, 2, 44, 45, 57]. Joint-embedding predictive architectures (JEPA) [4, 7, 10, 11, 41] align temporally adjacent representations in latent space.

**Video event understanding** has primarily treated temporal structure as a flat labeling problem, assigning each frame or segment to a single action category. Early approaches used structured temporal models such as HMMs and CRFs [12, 37], while modern methods employ temporal convolutional networks [21, 39], transformers [22, 64], or graph-based architectures [28, 61] to predict frame-wise actions or segment boundaries. Large-scale benchmarks such as Breakfast Actions [36], 50 Salads [54], EpicKitchens [17, 18], Ego4D [24], and Assembly101 [51] have driven rapid progress, along with task variants including action localization [1, 2, 44, 57], procedure segmentation [8, 9, 31, 69], and Generic Event Boundary Detection (GEBD) [34, 53, 63]. Yet, these methods largely assume a flat temporal hierarchy, where each frame belongs to one independent class, ignoring the compositional structure that organizes human activity. Even “hierarchical” variants that stack models across scales [45, 49] rely on discrete label taxonomies rather than continuous predictive dynamics. Moreover, nearly all are offline, requiring full-video access before segmentation, limiting their adaptability to streaming or interactive scenarios.

**Partonomic structure** conceptualizes video understanding as uncovering the nested subevents and containment relations through which activities unfold. Spatial partonomies have been deeply explored in vision, but temporal partonomies remain understudied. Object-centric methods leverage spatial part-whole decompositions for robust recognition and reasoning [14, 16, 26, 29, 40, 50, 52, 70], while semantic segmentation [6, 60, 67] and scene-graph frameworks [30, 33, 35] capture hierarchical relations among entities within a scene. Extending such insights to the *temporal domain*, where events evolve, overlap, and causally interact, remains an open challenge. Temporal partonomy requires more than boundary detection; it entails identifying *structural containment*, understanding how short, motoric actions compose into longer activities and goals. *PARSE* bridges this gap by learning part-whole hierarchies directly from streaming prediction-error dynamics, producing temporally aligned, multi-scale representations that reflect the latent organization of real-world activities.

### 3. Partonomies: Hierarchical Event Structures

A *partonomy* captures how complex activities unfold across multiple temporal and semantic scales. Unlike taxonomies, which express *is-a* relationships among symbolic categories, partonomies encode *has-part* relationships among temporally extended subevents that collectively constitute a coherent whole [58]. This representation provides a bridge between low-level perceptual dynamics and high-level task structure, offering a foundation for modeling human-like understanding of long-horizon behavior [59, 65, 66].

Formally, we define a partonomy as a hierarchy of temporally ordered event segments  $\mathcal{P} = \{L_1, L_2, \dots, L_N\}$ , where each level  $L_i = \{e_1^{(i)}, e_2^{(i)}, \dots, e_{M_i}^{(i)}\}$  consists of disjoint intervals  $e_j^{(i)} = [s_j^{(i)}, t_j^{(i)}]$ , where  $s_j^{(i)}$  and  $t_j^{(i)}$  denote its start and end frame indices, respectively. Each higher-level event aggregates contiguous lower-level events, enforcing *temporal containment*, as defined by

$$\mathcal{C}(e_k^{(i+1)}) = \{e_j^{(i)} \in L_i \mid s_k^{(i+1)} \leq s_j^{(i)} < t_j^{(i)} \leq t_k^{(i+1)}\}. \quad (1)$$

where  $\forall e_k^{(i+1)} \in L_{i+1}$ , the operator  $\mathcal{C}(\cdot)$  returns its temporally contained children from level  $L_i$ . This containment induces a partial order  $e_a^{(i)} \prec e_b^{(i+1)}$  denoting that  $e_a^{(i)}$  is a constituent of  $e_b^{(i+1)}$ , forming a tree-structured decomposition of time. A valid partonomy therefore satisfies two key properties: (i) *structural coherence*, ensuring consistent parent-child relationships across levels, and (ii) *temporal compositionality*, ensuring that event boundaries are hierarchically aligned rather than independent across scales.

This multiscale organization parallels hierarchical theories of cortical perception, where higher layers integrate evidence over longer timescales while providing contextual feedback to lower ones. From a computational standpoint, such a hierarchy supports *predictive abstraction*: each level refines its internal hypothesis about ongoing activity through both feedforward evidence and feedback correction, producing a temporally structured representation that is robust to uncertainty, occlusion, and variation. Figure 1 illustrates an example partonomy for an everyday routine task such as *making breakfast*. Fine-grained motor *actions* (*reach cabinet, pour milk*) correspond to level  $L_1$ , mid-level *activities* (*take bowl, make cereal*) to level  $L_2$ , and *goal-oriented subroutines* (*prepare breakfast*) to level  $L_3$ , all nested within higher-level tasks (*morning routine, daily schedule*) at level  $L_4$ . Each higher layer subsumes multiple temporally contained subevents, capturing both the hierarchical structure and dynamics of human activity. In this work, we address the problem of *extracting such hierarchical partonomies directly from streaming video*, without supervision or predefined symbolic labels. Unlike prior approaches [30, 44, 45], we consider the *online, predictive* setting in which an agent must infer the evolving structure

of events incrementally as new visual evidence arrives. This formulation poses unique challenges: the model must anticipate forthcoming transitions while maintaining temporal consistency across abstraction levels.

#### 4. PARSE: Hierarchical Partonomy Extraction

We model the emergence of hierarchical partonomies as the natural outcome of predictive learning under uncertainty. Intuitively, an intelligent agent observing a video stream should continually anticipate future perceptual states, compare its predictions against reality, and reorganize its internal temporal representation when prediction errors exhibit sustained deviations. Such deviations correspond to event boundaries, i.e., moments where the predictive model must reconfigure its internal hypotheses. We model this as a hierarchical predictive learning framework where each predictive layer generates expectations about the layer below, receives prediction-error feedback, and updates its state only when error signals exceed adaptive thresholds. Trained under the streaming (causal) constraint, this hierarchy learns a continually evolving segmentation of time, a *partonomy of experience*, that mirrors human perception of events as nested, temporally bounded processes. Figure 2 visualizes this mechanism, showing how hierarchical prediction, transient error dynamics, and the resulting nested event structure arise from a single unified objective.

Let the incoming video be a sequence of frames  $\{x_t\}_{t=1}^T$ , with visual features  $f_t = \phi(x_t)$  extracted by a visual feature encoder  $\phi$ . The predictive hierarchy consists of  $N$  recurrent modules  $\{\mathcal{F}^{(1)}, \mathcal{F}^{(2)}, \dots, \mathcal{F}^{(N)}\}$ , each maintaining an internal hidden state  $h_t^{(i)}$  that evolves at its own temporal granularity. At every step, the system jointly minimizes the total predictive energy

$$\mathcal{E} = \sum_{i=1}^N \left( \mathcal{L}_{\text{pred}}^{(i)} + \lambda_s \mathcal{L}_{\text{sparse}}^{(i)} \right) \quad (2)$$

where  $\lambda_s$  balances the influence of sparsity regularization. During streaming inference, the per-level prediction errors  $\mathcal{L}_{\text{pred}}^{(i)}(t)$  form temporal traces whose transient peaks signal structural changes in the input. These error traces provide cues for hierarchical event segmentation and partonomy construction, avoiding the need for supervision or an explicit differentiable loss term.

##### 4.1. Hierarchical Predictive Dynamics

Each layer in the predictive hierarchy operates as a recurrent coding unit that maintains both a *local temporal hypothesis* and a *contextual prior* from higher layers. The hierarchical dynamics are designed to instantiate a computational analogue of predictive coding with episodic feedback: each level anticipates the evolution of its subordinate

representations while continually contextualizing them using the recent memory of higher-level states. This allows the model to infer nested temporal boundaries in a streaming fashion by implicitly tracking the evolving partonomy of ongoing experience. The lowest level,  $L_1$ , models fast, motion-driven transitions in the visual stream, i.e., those corresponding to short, motoric sub-events. Its hidden state evolves as a Markovian recurrence conditioned on both its previous representation and the incoming frame features:

$$h_{t+1}^{(1)} = \mathcal{F}^{(1)}(h_t^{(1)}, f_t), \quad (3)$$

where  $\mathcal{F}^{(1)}$  is a recurrent predictor (e.g., RNN or LSTM [27]) that learns local temporal dependencies. Higher levels evolve more slowly, integrating over extended horizons to form stable representations of mid- and high-level activities. Rather than depending only on the immediate lower-layer state  $h_t^{(i-1)}$ , each level  $L_i$  contextualizes its predictions using a trailing memory of the past  $K$  hidden states from the layer above,  $\{h_{t-k}^{(i+1)}\}_{k=1}^K$ . This design introduces a mechanism for top-down temporal contextualization, where higher-level hypotheses guide perception and segmentation at lower scales, analogous to goal-driven constrained event parsing in cognitive models of event perception [58, 59, 65].

Formally, the forward estimate produced by layer  $L_i$  for the next state of its subordinate layer  $L_{i-1}$  is given by:

$$\hat{h}_{t+1}^{(i-1)} = \mathcal{F}^{(i)}\left(h_t^{(i-1)}, \text{Attn}\left(h_t^{(i)}, \{h_{t-k}^{(i+1)}\}_{k=1}^K\right)\right) \quad (4)$$

where  $i \in [2, N]$  and  $\text{Attn}(\cdot)$  denotes a scaled dot-product attention operator:  $\text{Attn}(q, M) = \text{softmax}\left(\frac{qM^\top}{\sqrt{d}}\right)M$ , where  $q = h_t^{(i)}$ ,  $M = \{h_{t-k}^{(i+1)}\}_{k=1}^K$ , and  $d$  the embedding dimension. This mechanism adaptively weights recent higher-level hypotheses, enabling each layer to interpret local changes in light of its inferred position within a broader temporal context. The level-wise prediction loss compares the predictor’s output to the appropriate next-step target-frame features at the bottom level and the lower-level hidden state otherwise. Let

$$s_{t+1}^{(i-1)} = \begin{cases} f_{t+1}, & i = 1, \\ h_{t+1}^{(i-1)}, & i \geq 2, \end{cases} \quad \hat{s}_{t+1}^{(i-1)} = \mathcal{F}^{(i)}(\cdot). \quad (5)$$

The prediction loss at level  $i$  is then defined as the normalized sum-squared error

$$\mathcal{L}_{\text{pred}}^{(i)} = \frac{1}{d_{i-1}} \|\hat{s}_{t+1}^{(i-1)} - s_{t+1}^{(i-1)}\|_2^2, \quad (6)$$

where  $d_{i-1}$  denotes the dimensionality of  $s_{t+1}^{(i-1)}$ . Minimizing this hierarchical loss drives a dual process of inference and anticipation. Lower layers learn to predict short-term

visual dynamics, while upper layers evolve more slowly, forming temporally abstract hypotheses that serve as contextual priors. The attention-mediated top-down flow provides adaptive feedback, comparable to *partonomy consultation* in Event Segmentation Theory (EST) [58, 59, 65, 66], allowing the model to re-evaluate its segmentation hypotheses based on longer-term structural expectations. This interaction between bottom-up evidence accumulation and top-down partonomic context enables the system to form temporally aligned, multi-scale representations, capturing immediate perceptual regularities and long-range event perception.

**Sparsity and Temporal Smoothness.** Although  $\mathcal{L}_{\text{pred}}$  encourages predictive accuracy, it can overfit to transient noise, producing unstable latent activations and overly frequent segmentation. To regularize the hidden dynamics, we introduce an activation sparsity prior as  $\mathcal{L}_{\text{sparse}}^{(i)} = |h_t^{(i)}|_1$ . This  $L_1$  penalty constrains the magnitude of hidden activations, encouraging compact, energy-efficient representations punctuated by sparse bursts of activity that mark significant state changes. From an information-theoretic standpoint, it minimizes representational entropy, reducing spurious oscillations while retaining high sensitivity to meaningful transitions. Empirically, this term stabilizes hierarchical training and ensures that higher layers evolve more slowly, capturing progressively coarser abstractions.

## 4.2. Generic Hierarchical Boundary Inference

When a structural change occurs in the environment, such as the onset of a new action, the local prediction error  $\mathcal{L}_{\text{pred}}^{(i)}(t)$  exhibits a sharp transient increase. We exploit this property to detect event boundaries directly from the temporal dynamics of prediction errors, without introducing an explicit differentiable loss term. Following streaming inference, each per-level error sequence is first smoothed using a short moving average (window size  $K=3$ ) and then differentiated twice to accentuate inflection points. Boundaries  $\mathcal{B}^{(i)}$  are extracted as local maxima of the doubly differentiated, smoothed prediction-error signal within a neighborhood of radius  $r_i$ , formally:

$$\mathcal{B}^{(i)} = \left\{ t \mid \Delta^2[\text{MA}(\mathcal{L}_{\text{pred}}^{(i)}, K)]_t > \Delta^2[\text{MA}(\mathcal{L}_{\text{pred}}^{(i)}, K)]_\tau, \forall \tau \in \mathcal{N}_{r_i}(t) \right\} \quad (7)$$

where  $\mathcal{N}_{r_i}(t)$  denotes a temporal neighborhood of radius  $r_i$  (set by doing a grid search over the range of  $0.1 \times \text{FPS}$  to  $2 \times \text{FPS}$  for each level of the prediction stack). This procedure yields sparse, temporally coherent boundary sets  $\{\mathcal{B}^{(1)}, \dots, \mathcal{B}^{(N)}\}$  corresponding to hypothesized transitions at progressively coarser temporal scales. Higher-level boundaries naturally emerge around sustained accumula-

tions of prediction error, aligning with coarser temporal structure and producing nested event partitions.

### 4.2.1. Emergent Partonomy Structure

As the model processes streaming input, the latent hierarchy self-organizes into a multiscale representation of ongoing activity. Each layer contributes a temporally segmented view of the sequence, and their alignment through containment induces a compositional structure:

$$\mathcal{P} = \{L_1, L_2, \dots, L_N\}, \quad L_i = \{e_1^{(i)}, \dots, e_{M_i}^{(i)}\},$$

where each segment  $e_j^{(i)}$  spans consecutive frames between adjacent boundaries in  $\mathcal{B}^{(i)}$ . Temporal containment between levels ensures that finer events aggregate consistently into coarser ones, forming a nested decomposition of the input stream. This emergent organization provides both interpretability and efficiency. Instead of predicting discrete symbolic labels, the model learns to segment continuous experience into hierarchically aligned temporal units, allowing downstream reasoning modules, e.g., affordance inference or plan recognition, to operate at an appropriate abstraction level. Because prediction, segmentation, and structural alignment are all consequences of minimizing the unified energy in Equation 2, the system requires no external supervision or task-specific boundaries.

**Implementation Details.** We use a frozen EfficientNet-B2 [55], pretrained on ImageNet [19], as our primary choice of visual encoder, while also experiment with ResNet-50 [25] and ViT/B32 [20]. An LSTM [27] is chosen as a recurrent predictor at each level, in a three-layer prediction stack. For top-down contextualization, each predictor attends at level  $L_i$  over the last  $K=5$  hidden states of the predictor at level  $L_{i+1}$ , maintained using a FIFO queue. The entire stack is trained simultaneously in a streaming manner over the training set of each dataset, once using the ADAM [5] optimizer with a learning rate of  $1e^{-3}$ . During inference, the learning rate is dropped to  $1e^{-6}$  to allow the model to adapt to changes within a video, but is reset to the trained weights between videos to prevent learning transfer across videos.  $\lambda_{\text{bound}}$  and  $\lambda_{\text{sparse}}$  are set to 1.0 and 0.1, respectively. The boundary predictions are obtained by applying a moving-average filter set to 20% of the video frame rate and identifying transient peaks within a sliding window of size  $(0.25 \times \text{FPS}, 1.25 \times \text{FPS}, 2.00 \times \text{FPS})$  for the three hierarchical levels (tuned per dataset via grid search). All models are trained on a workstation server with an AMD Threadripper 64-core processor, 512 GB RAM, and 4 NVIDIA RTX 6000 ADA, one video at a time for streaming training. More details in the supplementary.

Dataset	Model	Streaming	Oracle	TED	hF1
Breakfast Actions	Fixed Length	✓	✓	38.42	21.46
	K-Means	✗	✓	16.18	8.60
	Oracle K-Means	✗	✓*	16.58	9.27
	Hierarchical	✗	✓	33.35	22.60
	Streamer	✓	✗	18.72	8.68
	PARSE (Ours)	✓	✗	36.04	26.81
50 Salads	Fixed Length	✓	✓	54.33	25.73
	K-Means	✗	✓	6.87	2.70
	Oracle K-Means	✗	✓*	6.85	2.71
	Hierarchical	✗	✓	35.59	17.98
	Streamer	✓	✗	14.34	3.70
	PARSE (Ours)	✓	✗	20.65	10.76
Assembly 101	Fixed Length	✓	✓	27.66	21.10
	K-Means	✗	✓	10.85	5.42
	Oracle K-Means	✗	✓*	11.00	5.57
	Hierarchical	✗	✓	30.20	21.76
	Streamer	✓	✗	15.04	8.83
	PARSE (ours)	✓	✗	32.77	21.99

Table 1. Partonomy inference performance (%). “Streaming” indicates whether the method operates in a streaming (causal) setting. “Oracle” denotes whether the approach assumes access to dataset-specific priors, such as the average number of segments to expect or the average length of a segment. \* indicates ground truth usage.

## 5. Experimental Evaluation

**Datasets.** We evaluate *PARSE* on three benchmark datasets with multi-scale temporal annotations: (1) *Breakfast Actions* [36], 1,712 third-person videos of 10 breakfast routines annotated at action (fine) and activity (coarse) levels. We use 325 videos for training and 48 with dual-level labels for testing. (2) *50 Salads* [54], over 4 hours of egocentric videos of 25 participants preparing two salads each, with fine-grained (e.g., cut tomato) and coarse-grained (e.g., prepare ingredients) labels. We train on 30 and test on 20 clips. (3) *Assembly101* [51], 4,321 egocentric videos of toy-vehicle assembly and disassembly with frame-level fine/coarse annotations. We use 114 clips for training and 200 for evaluation. For all datasets, two-level ground-truth partonomies are constructed by nesting fine-grained segments within their corresponding coarse events, ensuring temporal containment and structural coherence (Eq. 1). The supplementary shows qualitative visualizations for deeper partonomies extracted by *PARSE*.

**Tasks and Metrics.** We assess both temporal and structural fidelity through two complementary tasks: (i) *Hierarchical Generic Event Boundary Detection (H-GEBD)* measures how well prediction-error transients align with annotated boundaries across scales. Following prior GEBD protocols, we report precision, recall, and mean-IoU within a

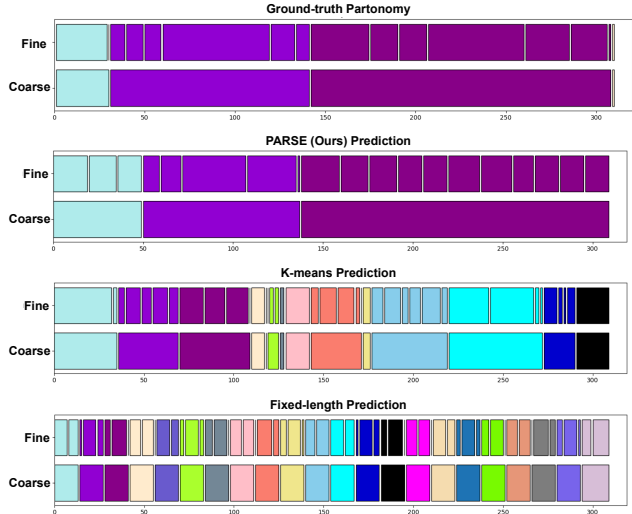


Figure 3. **Qualitative comparison of hierarchical partonomy predictions.** We visualize the two best-matching levels (fine and coarse) from each predicted hierarchy for a video “Making coffee” from Breakfast Actions. *PARSE* produces temporally coherent and hierarchically consistent segments.

temporal tolerance window. (ii) *Partonomy Structure Prediction* evaluates hierarchical consistency using Tree Edit Distance (TED) and hierarchical F1 (hF1). TED quantifies the cost of transforming the predicted hierarchy into the ground truth, while hF1 measures temporal alignment of corresponding segments across levels. Together, these metrics reflect the objectives in Eq. 2, where  $\mathcal{L}_{\text{pred}}$  governs temporal precision and  $\mathcal{L}_{\text{sparse}}$  and  $\mathcal{L}_{\text{bound}}$  regularize hierarchical structure. Full definitions are in the Supplementary.

**Baselines.** We compare against streaming and offline methods differing in temporal granularity and structural priors. *Fixed Length* divides each video into uniform-duration segments based on dataset-level averages. *K-means* clusters frame-level features into the average number of events per hierarchy level, while *K-means (Oracle)* uses ground-truth event counts per video as an upper bound. *Hierarchical Linkage* forms a temporal dendrogram over frame embeddings and extracts two-level partonomies by cutting at dataset-average event counts. *STREAMER* [45] is a transformer-based predictive baseline that trains layers sequentially, adding cross-layer communication after each stage to output boundary predictions per scale. *PARSE* is our proposed, unsupervised hierarchical predictive learner that operates fully online, jointly optimizing all layers under streaming constraints. All baselines use the same visual encoder (EfficientNetv2) for fairness.

### 5.1. Event Partonomy Prediction Performance

Table 1 reports quantitative results for the partonomy prediction task using the Tree Edit Distance (TED) and hier-

Dataset	Model	Streaming	Oracle	Fine-grained				Coarse-grained			
				Precision	Recall	mIoU	F1	Precision	Recall	mIoU	F1
Breakfast Actions	Fixed Length	✓	✓	22.11	26.56	13.44	24.13	8.95	25.78	6.45	13.29
	K-means	✗	✓	14.23	<b>66.67</b>	12.97	23.45	4.24	<b>75.88</b>	4.14	8.03
	Oracle K-means	✗	✓*	14.39	64.59	12.97	23.54	4.30	75.70	4.20	8.14
	Hierarchical	✗	✓	21.61	43.04	16.36	28.77	9.82	48.85	8.62	16.35
	Streamer	✓	✗	14.17	40.90	11.13	21.05	5.50	42.49	4.18	9.74
	PARSE (ours)	✓	✗	<b>22.48</b>	58.57	<b>18.93</b>	<b>32.49</b>	<b>13.61</b>	34.28	<b>10.98</b>	<b>19.48</b>
50 Salads	Fixed Length	✓	✓	<b>6.29</b>	5.77	3.10	6.02	3.80	5.57	2.31	4.52
	K-means	✗	✓	2.68	41.60	2.57	5.04	1.69	57.23	1.67	3.28
	Oracle K-means	✗	✓*	2.75	42.19	2.64	5.16	1.75	<b>60.39</b>	1.73	3.40
	Hierarchical	✗	✓	5.42	13.09	4.00	7.67	4.65	21.19	3.97	7.63
	Streamer	✓	✗	4.77	34.70	4.35	8.39	1.50	25.90	1.44	2.84
	PARSE (ours)	✓	✗	5.66	<b>52.05</b>	<b>5.10</b>	<b>10.21</b>	<b>5.19</b>	24.53	<b>4.40</b>	<b>8.57</b>
Assembly 101	Fixed Length	✓	✓	20.07	22.27	11.57	21.11	5.81	21.99	4.31	9.19
	K-means	✗	✓	12.27	<b>70.41</b>	11.60	20.90	1.77	<b>79.10</b>	1.76	3.46
	Oracle K-means	✗	✓*	12.39	69.82	11.68	21.05	1.78	78.42	1.77	3.48
	Hierarchical	✗	✓	<b>26.54</b>	48.09	<b>20.42</b>	<b>34.20</b>	6.46	40.71	<b>5.78</b>	<b>11.15</b>
	Streamer	✓	✗	16.24	30.12	11.71	21.10	1.98	26.69	1.88	3.69
	PARSE (ours)	✓	✗	20.55	63.92	18.34	31.10	<b>7.25</b>	18.66	5.34	10.44

Table 2. Hierarchical GEBD performance. Fine-grained and Coarse-grained boundary metrics. “Streaming” indicates whether the method operates causally. PARSE consistently outperforms other streaming baselines or offers competitive performance to non-streaming ones.

archical F1 (hF1) metrics. These measures capture complementary properties of hierarchical segmentation: TED prioritizes structural integrity, i.e., how well predicted parent-child relations and containment are preserved, while hF1 reflects temporal alignment and consistency across abstraction levels. Because these objectives often trade off, higher values in one metric do not always correspond to superior segmentation quality. Across datasets, *PARSE* achieves the best overall balance of TED and hF1 among streaming (causal) methods, consistently outperforming *STREAMER* and other non-oracle baselines. The *Fixed Length* baseline attains competitive TED scores on highly regular routines such as *Breakfast Actions* and *50 Salads*, where activity durations are approximately uniform; however, it fails under variable-length settings like *Assembly101*, where strict periodic segmentation violates temporal alignment. Clustering-based approaches (*K-means* and its oracle variant) and the *Hierarchical Linkage* method perform segmentation retrospectively: they require access to the entire video, rely on dataset- or ground-truth-derived heuristics (e.g., average event count or length), and construct paronomies post hoc. As a result, they cannot adapt to evolving uncertainty or streaming evidence. In contrast, *PARSE* operates fully online, discovering boundaries and adjusting hierarchical structure on the fly.

## 5.2. Hierarchical GEBD Performance

Table 2 reports the fine- and coarse-grained boundary detection results for all methods. This task emphasizes temporal segmentation fidelity rather than hierarchical structure, with precision and recall measuring selectivity and coverage of predicted transitions, and mIoU/F1 summarizing their alignment quality. In contrast to the structural TED-hF1 metrics in Table 1, these boundary-level measures are sensitive to over-segmentation and boundary drift, revealing the temporal stability of each approach. Across all datasets, *PARSE* achieves the highest or near-highest F1 and mIoU among streaming (causal) methods, demonstrating strong temporal coherence despite operating without access to future frames. The advantage is most evident on complex sequences such as *Breakfast Actions* and *Assembly101*, where boundary distributions are irregular and event durations vary widely. By coupling predictive anticipation with temporal smoothing, *PARSE* avoids the excessive fragmentation seen in *STREAMER* and the missed transitions characteristic of static segmentation methods. Offline baselines (*K-means*, *Hierarchical Linkage*) appear to achieve high recall or precision on certain datasets, but these results stem from retrospective access to the entire video and heuristic assumptions about event counts or durations. In contrast, *PARSE* infers boundaries directly from streaming prediction-error dynamics, adapting online to event variability and yielding consistent fine and coarse performance.

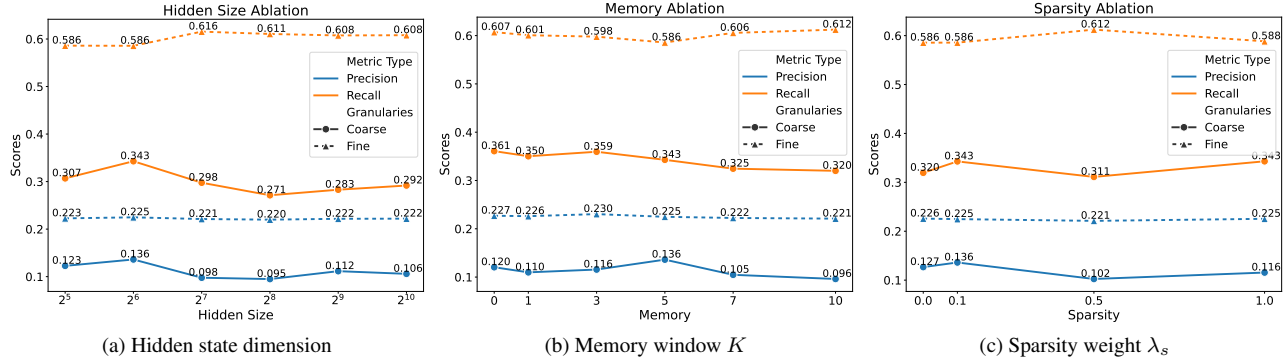


Figure 4. **Ablation on dynamic hyperparameters.** Effects of hidden-state size, top-down memory length, and sparsity regularization on boundary precision and recall at fine and coarse scales. Moderate configurations yield the most stable predictive dynamics.

Configuration	Fine F1	Coarse F1	TED	hF1
<i>Predictor Model</i>				
LSTM	<b>32.49</b>	<b>19.48</b>	<b>36.04</b>	<b>26.81</b>
Transformer	32.31	18.12	34.85	24.34
<i>Visual Encoder</i>				
EfficientNet-B2	<b>32.49</b>	<b>19.48</b>	<b>36.04</b>	<b>26.81</b>
ResNet-50	32.37	18.99	35.75	26.53
ViT/B-32	32.32	13.97	34.76	24.49
<i>Number of Prediction Layers</i>				
2 Layers	32.34	18.46	34.96	24.16
3 Layers	32.49	<b>19.48</b>	<b>36.04</b>	<b>26.81</b>
4 Layers	32.75	16.39	34.38	23.11
5 Layers	<b>33.26</b>	18.82	35.24	24.25

Table 3. Architectural ablations on the type of predictor at each layer, the visual backbone, and prediction hierarchy depth. Metrics are reported on the Breakfast Actions Dataset.

**Qualitative Discussion** Figure 3 illustrates representative two-level partonomies for the ground truth and different models. *PARSE* closely replicates the hierarchical organization of real activities, producing temporally coherent segments whose fine-level events remain properly contained within their corresponding coarse events. In contrast, most baselines, particularly *Fixed Length* and *K-means*, violate this containment constraint, as their recursive hierarchy construction often produces misaligned or fragmented boundaries across levels. These violations manifest as color discontinuities and inconsistent coarse-fine segmentation, revealing that static or clustering-based approaches cannot maintain temporal nesting when operating independently at each level. *PARSE*, by contrast, infers boundaries directly from hierarchical prediction-error dynamics, yielding partonomies that adapt naturally to event duration.

### 5.3. Ablation Studies

**Architectural choices.** As shown in Table 3, *PARSE* is robust across predictor types and visual backbones. Replacing the LSTM predictor with a Transformer yields similar performance but slightly weaker coarse-scale alignment, suggesting that recurrent gating better preserves temporal continuity under streaming constraints. Among encoders, EfficientNet-B2 achieves the highest overall consistency (TED = 36.0, hF1 = 26.8), while ResNet-50 and ViT/B-32 perform comparably despite differing in spatial bias. Varying the number of predictive layers reveals that three layers offer the best trade-off between temporal precision and structural depth: deeper hierarchies show minor gains in fine-grained recall but reduced hierarchical coherence.

**Dynamic hyperparameters.** Figure 4 examines the effect of sparsity weight  $\lambda_s$ , hidden-state dimension  $d_h$ , and memory window length  $K$  on both boundary and structural metrics. Moderate sparsity ( $\lambda_s=0.1$ ) consistently yields the highest coarse-level and partonomy scores. Lower values cause dense, unstable activations, whereas larger weights suppress adaptive changes, leading to under-segmentation. Hidden-state size shows a similar trend: increasing  $d_h$  up to 64 improves representational capacity, but further enlargement reduces coarse-level consistency due to oversmoothing. Memory window  $K=5$  performs best, balancing short-term responsiveness with long-range contextualization.

## 6. Discussion, Limitations, and Future Work

This paper introduced *PARSE*, a unified hierarchical predictive framework that learns multiscale event structure directly from streaming video without supervision or dataset-specific priors. By coupling predictive anticipation with sparsity-driven temporal regularization, *PARSE* infers coherent partonomies whose fine- and coarse-level boundaries emerge naturally from the dynamics of prediction error. Quantitative and qualitative evaluations across three datasets demonstrate that the model achieves competitive

structural and temporal alignment while operating entirely online. While promising, our formulation remains limited by the granularity and reliability of existing hierarchical annotations and by the scale of available training data. In the future, we aim to extend PARSE to richer datasets, continuous long-horizon streams, and more expressive (and deeper) event structures to better capture compositional structure in real-world tasks for embodied event perception.

**Acknowledgments.** This work was supported in part by the US NSF grants IIS 2348689 and IIS 2348690, and the USDA award no. 2023-69014-39716. The authors would like to thank the authors of the Breakfast Actions, Assembly-101, and 50-Salads for making their data and annotations publicly available.

## References

- [1] Sathyanarayanan Aakur and Sudeep Sarkar. Action localization through continual predictive learning. In *European conference on computer vision*, pages 300–317. Springer, 2020. 1, 3
- [2] Sathyanarayanan Aakur and Sudeep Sarkar. Actor-centered representations for action localization in streaming videos. In *European Conference on Computer Vision*, pages 70–87. Springer, 2022. 3
- [3] Sathyanarayanan N Aakur and Sudeep Sarkar. A perceptual prediction framework for self supervised event segmentation. In *Proceedings of the IEEE/CVF Conference on Computer Vision and Pattern Recognition*, pages 1197–1206, 2019. 1, 3
- [4] Mohamed Abdelfattah and Alexandre Alahi. S-jepa: A joint embedding predictive architecture for skeletal action recognition. In *European Conference on Computer Vision*, pages 367–384. Springer, 2024. 3
- [5] Kingma DP Ba J Adam et al. A method for stochastic optimization. *arXiv preprint arXiv:1412.6980*, 1412(6), 2014. 5
- [6] Pablo Arbeláez, Bharath Hariharan, Chunhui Gu, Saurabh Gupta, Lubomir Bourdev, and Jitendra Malik. Semantic segmentation using regions and parts. In *2012 IEEE Conference on Computer Vision and Pattern Recognition*, pages 3378–3385. IEEE, 2012. 3
- [7] Mahmoud Assran, Quentin Duval, Ishan Misra, Piotr Bojanowski, Pascal Vincent, Michael Rabbat, Yann LeCun, and Nicolas Ballas. Self-supervised learning from images with a joint-embedding predictive architecture. In *Proceedings of the IEEE/CVF Conference on Computer Vision and Pattern Recognition*, pages 15619–15629, 2023. 3
- [8] Siddhant Bansal, Chetan Arora, and CV Jawahar. My view is the best view: Procedure learning from egocentric videos. In *European Conference on Computer Vision*, pages 657–675. Springer, 2022. 3
- [9] Siddhant Bansal, Chetan Arora, and CV Jawahar. United we stand, divided we fall: Unitygraph for unsupervised procedure learning from videos. In *Proceedings of the IEEE/CVF Winter Conference on Applications of Computer Vision*, pages 6509–6519, 2024. 1, 3
- [10] Adrien Bardes, Quentin Garrido, Jean Ponce, Xinlei Chen, Michael Rabbat, Yann LeCun, Mido Assran, and Nicolas Ballas. V-jepa: Latent video prediction for visual representation learning. 2023. 3
- [11] Adrien Bardes, Jean Ponce, and Yann LeCun. Mc-jepa: A joint-embedding predictive architecture for self-supervised learning of motion and content features. *arXiv preprint arXiv:2307.12698*, 2023. 3
- [12] Siddhartha Chandra, Camille Couprie, and Iasonas Kokkinos. Deep spatio-temporal random fields for efficient video segmentation. In *Proceedings of the IEEE Conference on Computer Vision and Pattern Recognition*, pages 8915–8924, 2018. 3
- [13] Zhou Chen, Sanjoy Kundu, Harsimran S Baweja, and Sathyanarayanan N Aakur. Ease: Embodied active event perception via self-supervised energy minimization. *IEEE Robotics and Automation Letters*, 2025. 3
- [14] Jingchun Cheng, Yi-Hsuan Tsai, Wei-Chih Hung, Shengjin Wang, and Ming-Hsuan Yang. Fast and accurate online video object segmentation via tracking parts. In *IEEE Conference on Computer Vision and Pattern Recognition*, pages 7415–7424, 2018. 3
- [15] Andy Clark. Whatever next? predictive brains, situated agents, and the future of cognitive science. *Behavioral and brain sciences*, 36(3):181–204, 2013. 2
- [16] Alberto Crivellaro, Mahdi Rad, Yannick Verdie, Kwang Moo Yi, Pascal Fua, and Vincent Lepetit. Robust 3d object tracking from monocular images using stable parts. *IEEE Transactions on Pattern Analysis and Machine Intelligence*, 40(6): 1465–1479, 2017. 3
- [17] Dima Damen, Hazel Doughty, Giovanni Maria Farinella, Sanja Fidler, Antonino Furnari, Evangelos Kazakos, Davide Moltisanti, Jonathan Munro, Toby Perrett, Will Price, et al. Scaling egocentric vision: The epic-kitchens dataset. In *Proceedings of the European conference on computer vision (ECCV)*, pages 720–736, 2018. 3
- [18] Dima Damen, Hazel Doughty, Giovanni Maria Farinella, Sanja Fidler, Antonino Furnari, Evangelos Kazakos, Davide Moltisanti, Jonathan Munro, Toby Perrett, Will Price, et al. The epic-kitchens dataset: Collection, challenges and baselines. *IEEE Transactions on Pattern Analysis and Machine Intelligence*, 43(11):4125–4141, 2020. 3
- [19] Jia Deng, Wei Dong, Richard Socher, Li-Jia Li, Kai Li, and Li Fei-Fei. Imagenet: A large-scale hierarchical image database. In *2009 IEEE Conference on Computer Vision and Pattern Recognition*, pages 248–255. Ieee, 2009. 5
- [20] Alexey Dosovitskiy, Lucas Beyer, Alexander Kolesnikov, Dirk Weissenborn, Xiaohua Zhai, Thomas Unterthiner, Mostafa Dehghani, Matthias Minderer, Georg Heigold, Sylvain Gelly, et al. An image is worth 16x16 words: Transformers for image recognition at scale. In *International Conference on Learning Representations*, 2021. 5
- [21] Yazan Abu Farha and Jurgen Gall. Ms-tcn: Multi-stage temporal convolutional network for action segmentation. In *Proceedings of the IEEE/CVF Conference on Computer Vision and Pattern Recognition*, pages 3575–3584, 2019. 3
- [22] Mohsen Fayyaz and Jurgen Gall. Sct: Set constrained temporal transformer for set supervised action segmentation. In

- Proceedings of the IEEE/CVF Conference on Computer Vision and Pattern Recognition*, pages 501–510, 2020. 1, 3
- [23] Karl Friston. The free-energy principle: a unified brain theory? *Nature reviews neuroscience*, 11(2):127–138, 2010. 2
- [24] Kristen Grauman, Andrew Westbury, Eugene Byrne, Zachary Chavis, Antonino Furnari, Rohit Girdhar, Jackson Hamburger, Hao Jiang, Miao Liu, Xingyu Liu, et al. Ego4d: Around the world in 3,000 hours of egocentric video. In *Proceedings of the IEEE/CVF Conference on Computer Vision and Pattern Recognition*, pages 18995–19012, 2022. 3
- [25] Kaiming He, Xiangyu Zhang, Shaoqing Ren, and Jian Sun. Deep residual learning for image recognition. In *Proceedings of the IEEE Conference on Computer Vision and Pattern Recognition*, pages 770–778, 2016. 5
- [26] Bernd Heisele, Thomas Serre, Massimiliano Pontil, Thomas Vetter, and Tomaso A Poggio. Categorization by learning and combining object parts. In *Advances in Neural Information Processing Systems*, pages 1239–1245, 2001. 3
- [27] Sepp Hochreiter and Jürgen Schmidhuber. Long short-term memory. *Neural Computation*, 9(8):1735–1780, 1997. 4, 5
- [28] Yifei Huang, Yusuke Sugano, and Yoichi Sato. Improving action segmentation via graph-based temporal reasoning. In *Proceedings of the IEEE/CVF Conference on Computer Vision and Pattern Recognition*, pages 14024–14034, 2020. 1, 3
- [29] Daniel Huber, Anuj Kapuria, Raghavendra Donamukkala, and Martial Hebert. Parts-based 3d object classification. In *IEEE Conference on Computer Vision and Pattern Recognition*, pages II–II. IEEE, 2004. 3
- [30] Jingwei Ji, Ranjay Krishna, Li Fei-Fei, and Juan Carlos Niebles. Action genome: Actions as compositions of spatio-temporal scene graphs. In *Proceedings of the IEEE/CVF Conference on Computer Vision and Pattern Recognition*, pages 10236–10247, 2020. 3
- [31] Lei Ji, Chenfei Wu, Daisy Zhou, Kun Yan, Edward Cui, Xilin Chen, and Nan Duan. Learning temporal video procedure segmentation from an automatically collected large dataset. In *Proceedings of the IEEE/CVF Winter Conference on Applications of Computer Vision*, pages 1506–1515, 2022. 3
- [32] Linxing Preston Jiang and Rajesh PN Rao. Dynamic predictive coding explains both prediction and postdiction in visual motion perception. In *Proceedings of the Annual Meeting of the Cognitive Science Society*, 2023. 2
- [33] Justin Johnson, Ranjay Krishna, Michael Stark, Li-Jia Li, David Shamma, Michael Bernstein, and Li Fei-Fei. Image retrieval using scene graphs. In *Proceedings of the IEEE Conference on Computer Vision and Pattern Recognition*, pages 3668–3678, 2015. 3
- [34] Hyungrok Jung, Daneul Kim, Seunggyun Lim, Jeany Son, and Jonghyun Choi. Online generic event boundary detection. In *Proceedings of the IEEE/CVF International Conference on Computer Vision*, pages 13741–13750, 2025. 3
- [35] Ranjay Krishna, Yuke Zhu, Oliver Groth, Justin Johnson, Kenji Hata, Joshua Kravitz, Stephanie Chen, Yannis Kalantidis, Li-Jia Li, David A Shamma, et al. Visual genome: Connecting language and vision using crowdsourced dense image annotations. *International Journal of Computer Vision*, 123(1):32–73, 2017. 3
- [36] Hilde Kuehne, Ali Arslan, and Thomas Serre. The language of actions: Recovering the syntax and semantics of goal-directed human activities. In *Proceedings of the IEEE Conference on Computer Vision and Pattern Recognition*, pages 780–787, 2014. 1, 2, 3, 6, 13
- [37] Hilde Kuehne, Alexander Richard, and Juergen Gall. A hybrid rnn-hmm approach for weakly supervised temporal action segmentation. *IEEE transactions on pattern analysis and machine intelligence*, 42(4):765–779, 2018. 3
- [38] Sateesh Kumar, Sanjay Haresh, Awais Ahmed, Andrey Konin, M. Zeeshan Zia, and Quoc-Huy Tran. Unsupervised action segmentation by joint representation learning and online clustering. In *Proceedings of the IEEE/CVF Conference on Computer Vision and Pattern Recognition (CVPR)*, pages 20174–20185, 2022. 1
- [39] Colin Lea, Michael D Flynn, Rene Vidal, Austin Reiter, and Gregory D Hager. Temporal convolutional networks for action segmentation and detection. In *proceedings of the IEEE Conference on Computer Vision and Pattern Recognition*, pages 156–165, 2017. 3
- [40] Bastian Leibe, Alan Ettl, and Bernt Schiele. Learning semantic object parts for object categorization. *Image and Vision Computing*, 26(1):15–26, 2008. 3
- [41] Etai Littwin, Omid Saremi, Madhu Advani, Vimal Thilak, Preetum Nakkiran, Chen Huang, and Joshua Susskind. How jepa avoids noisy features: The implicit bias of deep linear self distillation networks. *Advances in Neural Information Processing Systems*, 37:91300–91336, 2024. 3
- [42] William Lotter, Gabriel Kreiman, and David Cox. Deep predictive coding networks for video prediction and unsupervised learning. In *International Conference on Learning Representations*, 2017. 2
- [43] Gary Lupyan and Andy Clark. Words and the world: Predictive coding and the language-perception-cognition interface. *Current Directions in Psychological Science*, 24(4): 279–284, 2015. 2
- [44] Ramy Mounir, Ahmed Shahabaz, Roman Gula, Jörn Theuerkauf, and Sudeep Sarkar. Towards automated ethogramming: Cognitively-inspired event segmentation for streaming wildlife video monitoring. *International Journal of Computer Vision*, (9), 2023. 1, 3
- [45] Ramy Mounir, Sujal Vijayaraghavan, and Sudeep Sarkar. Streamer: Streaming representation learning and event segmentation in a hierarchical manner. *Advances in Neural Information Processing Systems*, 36:45694–45715, 2023. 1, 3, 6, 14
- [46] Rajesh PN Rao. A sensory-motor theory of the neocortex based on active predictive coding. *bioRxiv*, pages 2022–12, 2022. 2
- [47] Rajesh PN Rao, Dimitrios C Gklezacos, and Vishwas Sathish. Active predictive coding: A unifying neural model for active perception, compositional learning, and hierarchical planning. *Neural Computation*, 36(1):1–32, 2023. 2
- [48] Tommaso Salvatori, Ankur Mali, Christopher L Buckley, Thomas Lukasiewicz, Rajesh PN Rao, Karl Friston, and Alexander Ororbia. Brain-inspired computational intelligence via predictive coding. 2023. 2

- [49] Saquib Sarfraz, Naila Murray, Vivek Sharma, Ali Diba, Luc Van Gool, and Rainer Stiefelhagen. Temporally-weighted hierarchical clustering for unsupervised action segmentation. In *Proceedings of the IEEE/CVF Conference on Computer Vision and Pattern Recognition*, pages 11225–11234, 2021. 1, 3
- [50] Henry Schneiderman and Takeo Kanade. Object detection using the statistics of parts. *International Journal of Computer Vision*, 56(3):151–177, 2004. 3
- [51] Fadime Sener, Dibyadip Chatterjee, Daniel Shelepov, Kun He, Dipika Singhania, Robert Wang, and Angela Yao. Assembly101: A large-scale multi-view video dataset for understanding procedural activities. In *Proceedings of the IEEE/CVF Conference on Computer Vision and Pattern Recognition*, pages 21096–21106, 2022. 1, 2, 3, 6, 13
- [52] Shaoshuai Shi, Zhe Wang, Jianping Shi, Xiaogang Wang, and Hongsheng Li. From points to parts: 3d object detection from point cloud with part-aware and part-aggregation network. *IEEE Transactions on Pattern Analysis and Machine Intelligence*, 2020. 3
- [53] Mike Zheng Shou, Stan Weixian Lei, Weiyao Wang, Deepti Ghadiyaram, and Matt Feiszli. Generic event boundary detection: A benchmark for event segmentation. In *Proceedings of the IEEE/CVF international conference on computer vision*, pages 8075–8084, 2021. 1, 3
- [54] Sebastian Stein and Stephen J McKenna. Combining embedded accelerometers with computer vision for recognizing food preparation activities. In *Proceedings of the 2013 ACM International Joint Conference on Pervasive and Ubiquitous Computing*, pages 729–738, 2013. 2, 3, 6, 13
- [55] Mingxing Tan and Quoc Le. Efficientnetv2: Smaller models and faster training. In *International Conference on Machine Learning*, pages 10096–10106. PMLR, 2021. 5
- [56] Shubham Trehan and Sathyanarayanan N Aakur. Towards active vision for action localization with reactive control and predictive learning. In *Proceedings of the IEEE/CVF Winter Conference on Applications of Computer Vision*, pages 783–792, 2022. 3
- [57] Shubham Trehan and Sathyanarayanan N Aakur. Self-supervised multi-actor social activity understanding in streaming videos. In *International Conference on Pattern Recognition*, pages 293–309. Springer, 2024. 3
- [58] Barbara Tversky. Where paronomies and taxonomies meet. In *Meanings and Prototypes (RLE Linguistics B: Grammar)*, pages 334–344. Routledge, 2014. 1, 2, 3, 4, 5
- [59] Barbara Tversky, Jeffrey M Zacks, and B Martin Hard. The structure of experience. *Understanding events: From perception to action*, pages 436–464, 2008. 1, 3, 4, 5
- [60] Panqu Wang, Pengfei Chen, Ye Yuan, Ding Liu, Zehua Huang, Xiaodi Hou, and Garrison Cottrell. Understanding convolution for semantic segmentation. In *2018 IEEE winter conference on applications of computer vision (WACV)*, pages 1451–1460. IEEE, 2018. 3
- [61] Tao Wang, Ning Xu, Kean Chen, and Weiyao Lin. End-to-end video instance segmentation via spatial-temporal graph neural networks. In *Proceedings of the IEEE/CVF international conference on computer vision*, pages 10797–10806, 2021. 1, 3
- [62] Xiao Wang, Jingen Liu, Tao Mei, and Jiebo Luo. Coseg: Cognitively inspired unsupervised generic event segmentation. *IEEE Transactions on Neural Networks and Learning Systems*, 35(9):12507–12517, 2023. 3
- [63] Yuxuan Wang, Difei Gao, Licheng Yu, Weixian Lei, Matt Feiszli, and Mike Zheng Shou. Geb+: A benchmark for generic event boundary captioning, grounding and retrieval. In *European Conference on Computer Vision*, pages 709–725. Springer, 2022. 1, 3
- [64] Fangqiu Yi, Hongyu Wen, and Tingting Jiang. As-former: Transformer for action segmentation. *arXiv preprint arXiv:2110.08568*, 2021. 1, 3
- [65] Jeffrey M Zacks and Barbara Tversky. Event structure in perception and conception. *Psychological Bulletin*, 127(1): 3, 2001. 1, 2, 3, 4, 5
- [66] Jeffrey M Zacks, Barbara Tversky, and Gowri Iyer. Perceiving, remembering, and communicating structure in events. *Journal of Experimental Psychology: General*, 130(1):29, 2001. 1, 3, 5
- [67] Hang Zhang, Kristin Dana, Jianping Shi, Zhongyue Zhang, Xiaogang Wang, Amrith Tyagi, and Amit Agrawal. Context encoding for semantic segmentation. In *Proceedings of the IEEE Conference on Computer Vision and Pattern Recognition*, pages 7151–7160, 2018. 3
- [68] Kaizhong Zhang and Dennis Shasha. Simple fast algorithms for the editing distance between trees and related problems. *SIAM journal on computing*, 18(6):1245–1262, 1989. 12
- [69] Honglu Zhou, Roberto Martín-Martín, Mubbasir Kapadia, Silvio Savarese, and Juan Carlos Niebles. Procedure-aware pretraining for instructional video understanding. In *Proceedings of the IEEE/CVF Conference on Computer Vision and Pattern Recognition*, pages 10727–10738, 2023. 3
- [70] Yousong Zhu, Chaoyang Zhao, Jinqiao Wang, Xu Zhao, Yi Wu, and Hanqing Lu. Couplenet: Coupling global structure with local parts for object detection. In *IEEE International Conference on Computer Vision*, pages 4126–4134, 2017. 3

## Appendix A

### 7. Evaluation Metrics and Protocols

We evaluate our model using two complementary tasks designed to measure both (i) the temporal accuracy of detected boundaries across abstraction levels and (ii) the structural correctness of the resulting partonomy. These correspond to the behavioral manifestations of the optimization objective in Equation 2: the predictive consistency term ( $\mathcal{L}_{\text{pred}}$ ) aligns with temporal precision and recall, while the sparsity ( $\mathcal{L}_{\text{sparse}}$ ) and boundary regularization ( $\mathcal{L}_{\text{bound}}$ ) shape the emergence of stable, hierarchically aligned structures. Together, they form the computational substrate for the two evaluation tasks described below.

#### 7.1. Hierarchical Generic Event Boundary Detection (H-GEED)

The first task assesses *temporal segmentation accuracy* at each level  $L_i$  of the predicted hierarchy. Let the predicted boundary set be  $\mathcal{B}_p^{(i)} = \{b_1, \dots, b_{M_p}\}$  and the ground-truth boundary set be  $\mathcal{B}_g^{(i)} = \{g_1, \dots, g_{M_g}\}$ . A predicted boundary  $b_k$  is considered correct if it lies within a tolerance window of  $\pm w$  frames around any ground-truth boundary:

$$\delta(b_k, \mathcal{B}_g^{(i)}) = \begin{cases} 1, & \exists g_j \in \mathcal{B}_g^{(i)} \text{ s.t. } |b_k - g_j| \leq w, \\ 0, & \text{otherwise.} \end{cases} \quad (8)$$

Using this criterion, we compute:

$$TP = \sum_k \delta(b_k, \mathcal{B}_g^{(i)}) \quad (9)$$

$$FP = M_p - TP, \quad FN = M_g - TP, \quad (10)$$

and define the standard metrics:

$$P = \frac{TP}{TP + FP} \quad (11)$$

$$R = \frac{TP}{TP + FN} \quad (12)$$

$$\text{mIoU} = \frac{TP}{TP + FP + FN}. \quad (13)$$

Precision ( $P$ ) measures the selectivity of boundary detections, recall ( $R$ ) quantifies the completeness of the segmentation, and mIoU measures the overlap consistency between predicted and ground-truth boundaries. Across levels, these scores reveal how the model’s hierarchical prediction errors translate into temporally aligned boundary transitions, thereby validating the effect of  $\mathcal{L}_{\text{pred}}$  and  $\mathcal{L}_{\text{bound}}$  in Equation 2.

#### 7.2. Partonomy Structure Prediction

While H-GEED evaluates boundary timing, it does not assess whether the predicted boundaries yield a coherent hierarchical structure. We therefore evaluate the emergent

partonomy  $\hat{\mathcal{P}} = \{\hat{L}_1, \hat{L}_2, \dots, \hat{L}_N\}$  against the ground truth  $\mathcal{P}^* = \{L_1^*, L_2^*, \dots, L_N^*\}$  using two complementary structural metrics: the *Tree Edit Distance (TED)* and the *Hierarchical F1-score (hF1)*.

**Tree Edit Distance (TED).** TED measures *structural correctness* by quantifying the minimal cost of transforming  $\hat{\mathcal{P}}$  into  $\mathcal{P}^*$  through insertions, deletions, or relabelings. Following [68], let each node correspond to an event segment  $e_j^{(i)}$ , and define the elementary edit operations:

$$\text{cost}(\text{insert}) = \alpha \quad (14)$$

$$\text{cost}(\text{delete}) = \alpha \quad (15)$$

$$\text{cost}(\text{relabel}) = \beta d_{\text{label}}(e_a, e_b), \quad (16)$$

where  $d_{\text{label}}$  is 1 for label mismatch and 0 otherwise. Since our task is unsupervised, we always set  $\beta = 0$  and  $\alpha = 1$ . The TED between the two partonomies is then defined recursively as

$$\text{TED}(\hat{\mathcal{P}}, \mathcal{P}^*) = \min_{\pi \in \Pi} \sum_{(a,b) \in \pi} \text{cost}(a \rightarrow b), \quad (17)$$

where  $\Pi$  is the set of all valid edit paths between corresponding trees. We normalize the TED by the total number of nodes to obtain a similarity score in  $[0, 1]$ :

$$\text{TED-Sim} = 1 - \frac{\text{TED}(\hat{\mathcal{P}}, \mathcal{P}^*)}{\alpha(|\hat{\mathcal{P}}| + |\mathcal{P}^*|)}. \quad (18)$$

A higher TED-Sim indicates better preservation of hierarchical structure and parent-child containment as defined in Equation 1.

**Hierarchical F1 (hF1).** While TED evaluates discrete structure, hF1 measures *temporal consistency* across abstraction levels. At each depth  $i$ , we first extract the set of segments  $L_i = \{e_1^{(i)}, \dots, e_{M_i}^{(i)}\}$  and  $\hat{L}_i = \{\hat{e}_1^{(i)}, \dots, \hat{e}_{\hat{M}_i}^{(i)}\}$ . For each pair  $(e_a^{(i)}, \hat{e}_b^{(i)})$ , we compute their intersection-over-union:

$$\text{IoU}(e_a^{(i)}, \hat{e}_b^{(i)}) = \frac{|e_a^{(i)} \cap \hat{e}_b^{(i)}|}{|e_a^{(i)} \cup \hat{e}_b^{(i)}|}. \quad (19)$$

We perform bipartite matching via the Hungarian algorithm to maximize total IoU, and count a match if  $\text{IoU} \geq \tau$ . The level-wise F1-score is then:

$$F_1^{(i)} = \frac{2P^{(i)}R^{(i)}}{P^{(i)} + R^{(i)}} \quad (20)$$

$$P^{(i)} = \frac{TP^{(i)}}{TP^{(i)} + FP^{(i)}}, \quad R^{(i)} = \frac{TP^{(i)}}{TP^{(i)} + FN^{(i)}}. \quad (21)$$

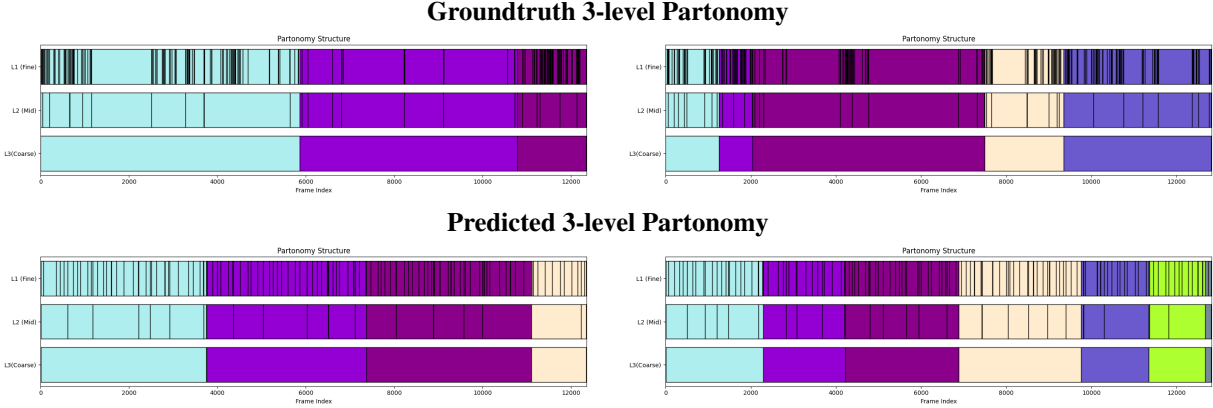


Figure 5. **Three-level partonomy predictions** for simulated long videos for subjects P44 and P48 from the Breakfast Actions dataset.

The overall hierarchical F1 is the mean across levels:

$$\text{hF1} = \frac{1}{N} \sum_{i=1}^N F_1^{(i)}. \quad (22)$$

High hF1 values indicate that predicted event boundaries not only align temporally with ground-truth segments but also respect the containment and ordering constraints across scales.

### 7.3. Interpretation

TED and hF1 together provide a complete picture of partonomy inference performance. TED reflects the *structural well-formedness* of the predicted hierarchy—how faithfully the model reconstructs the parent-child relationships between nested events. hF1 reflects the *temporal containment fidelity*—whether segment boundaries at different scales remain hierarchically consistent. These metrics complement the H-GEED measures from Eq. 13: while boundary-level precision and recall are sensitive to the temporal localization of change, TED and hF1 are sensitive to the *structural coherence* that emerges through minimizing the energy objective in Equation 2. Together, they evaluate whether the model not only predicts *when* event transitions occur but also *how* these transitions compose to form a temporally coherent, multiscale partonomy.

## 8. Detailed Experimental Setup

**Data.** We repurpose three publicly available datasets with multi-scale temporal annotations to evaluate our model on two tasks: (i) partonomy inference, which measures the recovery of nested event hierarchies, and (ii) hierarchical generic event boundary detection (H-GEED), which assesses temporal segmentation consistency across abstraction levels. Breakfast Actions [36] contains 1,712 third-person videos of 10 breakfast preparation activities per-

formed by 52 actors. Each video is annotated at both fine-grained (action) and coarse-grained (activity) levels, enabling two-level hierarchical evaluation. We use 48 videos with dual-level annotations for testing and sample 325 for training. 50 Salads [54] includes over 4 hours of egocentric recordings of 25 participants each preparing two mixed salads. Videos are annotated with both low-level action segments (e.g., cut tomato) and high-level activity labels (e.g., prepare ingredients). We evaluate on 20 videos containing both levels of annotation and train on 30 additional clips. Assembly101 [51] is a large-scale egocentric dataset comprising 4,321 videos of participants assembling and disassembling 101 toy vehicles with frame-level fine and coarse annotations. We sample 114 clips for training and 200 for evaluation. For all datasets, we construct two-level partonomies by recursively nesting fine-grained temporal segments within their corresponding coarse-grained segments. Empirically, we find that reliable ground-truth partonomies can be constructed up to two levels without violating temporal containment or structural coherence assumptions defined in Equation 1.

**Evaluation Tasks and Metrics.** We evaluate our model on two complementary tasks that jointly assess the temporal and structural fidelity of inferred partonomies. The first task, Hierarchical Generic Event Boundary Detection (H-GEED), measures how well transient prediction-error peaks align with annotated event transitions at multiple temporal scales. Following prior GEED formulations, we compute precision, recall, and mean-IoU between predicted and ground-truth boundary frames within a tolerance window, quantifying both selectivity and coverage of temporal change. The second task, Partonomy Structure Prediction, evaluates the hierarchical consistency of the inferred event tree using the Tree Edit Distance (TED) and the hierarchical F1-score (hF1). TED captures the structural cost of transforming the predicted hierarchy into the ground truth, re-

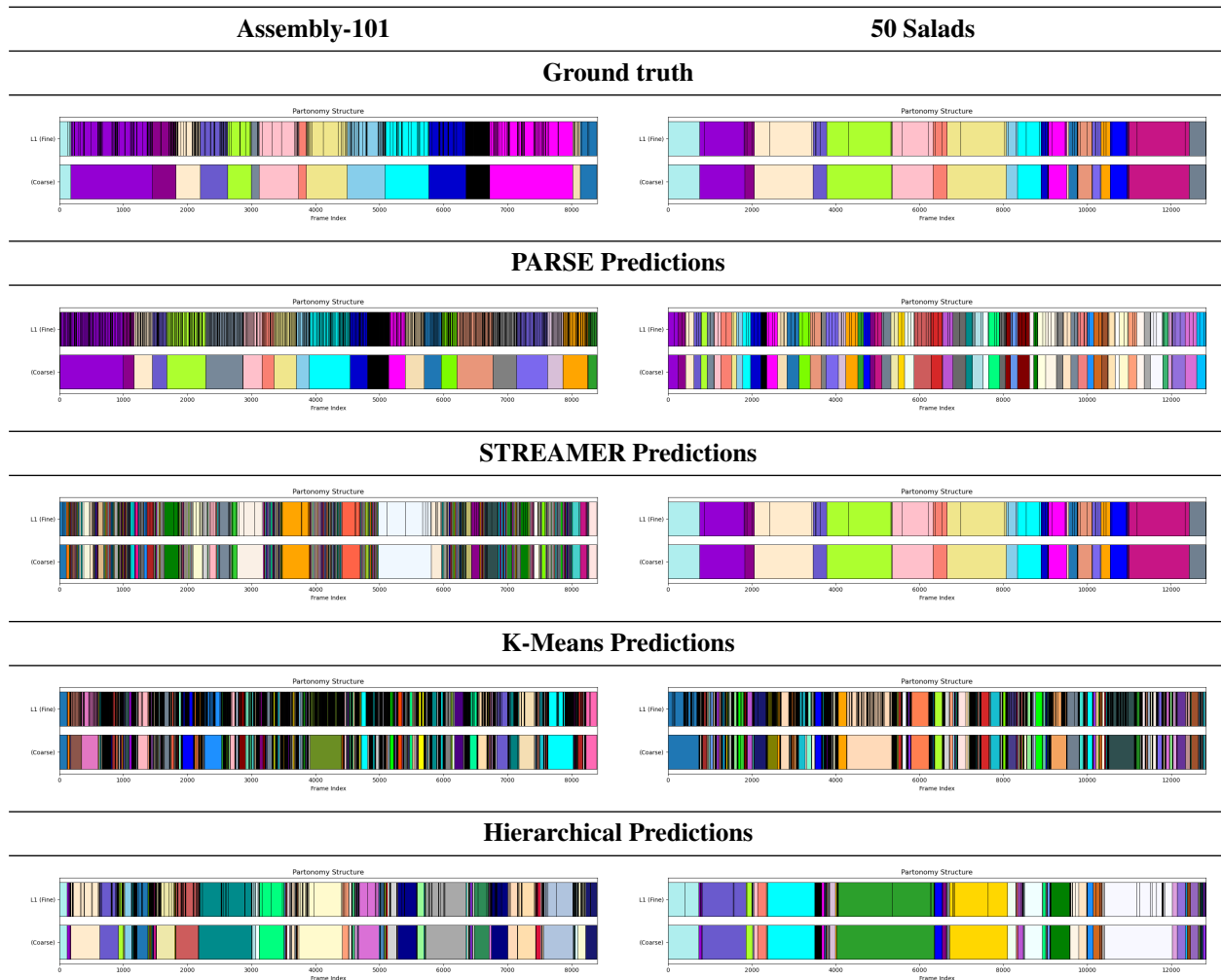


Figure 6. **Additional Qualitative Visualizations** of the predictions from different baselines on the Assembly-101 (left) and 50 Salads (right) datasets.

flecting parent–child containment and compositional coherence, while hF1 measures the temporal alignment of corresponding segments across levels using IoU-based matching. Together, these metrics directly evaluate the objectives encoded in Equation 2:  $\mathcal{L}_{\text{pred}}$  governs temporal precision and  $\mathcal{L}_{\text{sparse}}$  and  $\mathcal{L}_{\text{bound}}$  regulate hierarchical consistency. Full mathematical definitions of TED, hF1, and the boundary metrics are provided in the Supplementary.

**Baselines.** We compare our approach (*PARSE*) against a diverse set of streaming and offline segmentation baselines that differ in how they infer multi-scale temporal structure. *Fixed Length* constructs two-level partonomies by partitioning each video into segments of uniform duration, where the average segment length at each hierarchy level is estimated from dataset statistics. *K-means* uses the average number of events per level in each dataset as the target cluster count, performing feature clustering on frame-level visual

embeddings (identical to those used in our model) and recursively nesting the resulting segments into a two-level hierarchy. *K-means (Oracle)* follows the same procedure but sets the cluster count to the ground-truth number of events in each video, providing an upper bound on unsupervised clustering performance. *Hierarchical Linkage* constructs a fully connected temporal linkage matrix over frame embeddings and derives a two-level partonomy by cutting the dendrogram at levels corresponding to the average number of events per hierarchy level in the dataset. *STREAMER* [45] is a transformer-based predictive model conceptually related to ours: it trains layers sequentially in a bottom-up fashion, training the first layer for 10k steps, then incrementally adding higher layers with cross-layer communication for an additional 10k steps each, to produce event boundary predictions at multiple temporal scales. The final partonomy is then constructed recursively as with the other baselines.

*PARSE* provides a unified, end-to-end hierarchical predictive learner that jointly optimizes all layers under streaming constraints, producing temporally aligned and coherent paronomies without supervision or dataset-specific priors.

## 9. Beyond 2-layer Paronomy

This section provides a qualitative demonstration that *PARSE* extends naturally beyond the two-level hierarchies used in our main experiments. Although the Breakfast Actions dataset provides only fine and coarse annotations, several participants perform multiple distinct tasks across separate videos. We use this structure to approximate a third paronomy level corresponding to high-level goals.

**Three-level hierarchical test set.** For each participant, we identify all video instances that share the same participant ID and contain both fine and coarse annotations. These videos are concatenated in chronological order to create a single continuous sequence. The fine and coarse annotations associated with each original clip are also concatenated along the temporal dimension so that they remain aligned with the merged sequence. We then introduce a third annotation level, denoted L3, which records the boundaries between the original sub-videos in the concatenated sequence. Each L3 segment corresponds to one high-level task performed by that participant, for example preparing juice, preparing milk, or making a sandwich. The resulting hierarchy is:

- L1: fine-grained action segments such as reaching for an object or pouring ingredients,
- L2: mid-level activity segments composed of multiple actions, such as preparing milk or assembling a sandwich,
- L3: goal-level segments corresponding to each original video associated with the participant.

**Qualitative results.** Figure 5 shows ground truth and predicted three-level paronomies for one representative participant. Although this test scenario is synthetic and does not represent a naturally continuous recording, *PARSE* produces a coherent nested hierarchy across all three levels. L1 boundaries remain dense and responsive to short-term changes, L2 boundaries reflect coherent multi-action activities, and L3 boundaries align with the larger goal transitions induced by video concatenation. Even in this setting, the predicted segments naturally respect containment across levels, demonstrating that the hierarchical consistency encouraged by the predictive cascade generalizes beyond the two-level structures used in training.

**Limitations.** We do not provide a quantitative evaluation for this experiment because concatenated videos do not form a continuous real-world activity stream. Camera resets and scene changes at clip boundaries violate the assumptions underlying our paronomy definition. Nevertheless, these qualitative results illustrate that the predictive hierarchy can be extended to deeper structures without modifica-

tions to the architecture or additional supervision.

## 10. Qualitative Visualization

Additional qualitative visualizations are shown in Figure 6 on Assembly-101 and 50 Salads datasets. As can be seen, *PARSE* consistently produces stable, nested segments across datasets.

## 11. Detailed Implementation Details

### 11.1. Breakfast Actions

#### Hyperparameters for *PARSE*

##### Model Configuration

- LSTM hidden size: 64
- LSTM layers: 1

##### Training Configuration

- Learning rate:  $1 \times 10^{-3}$
- Sparsity weight: 0.1

##### Inference Configuration

- Learning rate:  $1 \times 10^{-6}$
- Sparsity weight: 0.1
- Sliding history windows:  $\{7, 15, 30\}$  for L2/L3/L4

##### Postprocessing

- Moving average smoothing:

$$\text{smooth}_{L2} = 4, \quad \text{smooth}_{L3} = 3, \quad \text{smooth}_{L4} = 2$$

- Transient peak orders:

$$\text{order}_{L2} = 4, \quad \text{order}_{L3} = 20, \quad \text{order}_{L4} = 30$$

#### Implementation Details for Baselines:

**Setting  $k$  for different granularities:** We parse the ground-truth annotations and remove non-informative events such as `SIL`. The average number of valid segments is computed separately for the fine- and coarse-level annotations. For the mid-level granularity, we define its segment count as the rounded average of these two values:

$$k_{\text{mid}} = \left\lceil \frac{k_{\text{coarse}} + k_{\text{fine}}}{2} \right\rceil.$$

Using this procedure, the final values employed in all clustering-based baselines are:

$$k_{\text{coarse}} = 6, \quad k_{\text{mid}} = 22, \quad k_{\text{fine}} = 38.$$

### 11.2. Assembly 101

#### Hyperparameters for *PARSE*:

##### Model Configuration

- LSTM hidden size: 128
- LSTM layers: 1

##### Training Configuration

- Learning rate:  $1 \times 10^{-3}$
- Sparsity weight: 0.1

#### Inference Configuration

- Learning rate:  $1 \times 10^{-5}$
- Sparsity weight: 0.1
- Sliding history windows: {7, 15, 30} for L2/L3/L4

#### Postprocessing

- Moving average smoothing:

$$\text{smooth}_{L_2} = 3, \quad \text{smooth}_{L_3} = 3, \quad \text{smooth}_{L_4} = 3$$

- Transient peak orders:

$$\text{order}_{L_2} = 4, \quad \text{order}_{L_3} = 30, \quad \text{order}_{L_4} = 60$$

#### Implementation Details for Baselines.

We follow the same procedure described in the Breakfast dataset. For this dataset, the resulting values are:

$$k_{\text{coarse}} = 26, \quad k_{\text{mid}} = 134, \quad k_{\text{fine}} = 242.$$

### 11.3. 50 Salads

#### Hyperparameters for PARSE:

##### Model Configuration

- LSTM hidden size: 512
- LSTM layers: 1

##### Training Configuration

- Learning rate:  $1 \times 10^{-3}$
- Sparsity weight: 0.1

##### Inference Configuration

- Learning rate:  $1 \times 10^{-6}$
- Sparsity weight: 0.1
- Sliding history windows: {7, 15, 30} for L2/L3/L4

#### Postprocessing

- Moving average smoothing:

$$\text{smooth}_{L_2} = 3, \quad \text{smooth}_{L_3} = 3, \quad \text{smooth}_{L_4} = 3$$

- Transient peak orders:

$$\text{order}_{L_2} = 4, \quad \text{order}_{L_3} = 20, \quad \text{order}_{L_4} = 45$$

#### Implementation Details for Baselines:

For this dataset, the values are:

$$k_{\text{coarse}} = 19, \quad k_{\text{mid}} = 36, \quad k_{\text{fine}} = 52.$$

### 11.4. Impact of Order on Performance

As shown in Figure 7, as the order parameter increases at the L2 level, fine-grained precision gradually improves while fine-grained recall drops sharply. In the context of argrextrema, a larger order value requires each boundary candidate to be a strict local maximum over a broader neighborhood. This makes the detector more conservative at the

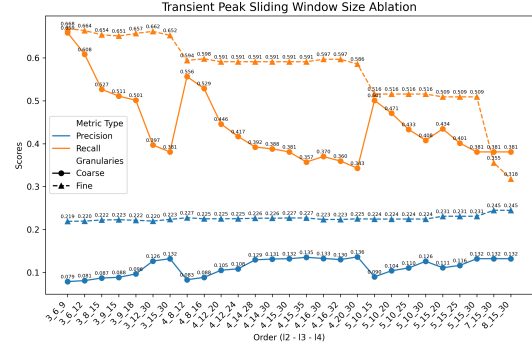


Figure 7. Ablation of the L2–L3–L4 order parameters on fine- and coarse-grained boundary detection, showing the precision–recall trade-off as the peak-detection neighborhood increases.

fine scale, suppressing many short-lived or weak peaks that would otherwise be considered boundaries.

A similar trend is observed when increasing the L3 and L4 orders: coarse-level precision consistently increases, whereas coarse-level recall steadily decreases. Since boundary events at these levels tend to be longer and smoother, requiring a larger neighborhood for peak validation further reduces the number of detected boundaries.

Overall, increasing the order parameter enforces stricter peak validation by expanding the neighborhood within which a point must dominate to be considered a boundary. This reduces the total number of predicted boundaries, resulting in higher precision (fewer false positives) but lower recall (more missed true transitions). The decline in recall is particularly pronounced at the fine level, where boundaries are shorter and more numerous, making them more sensitive to neighborhood enlargement.